Evolutionary dynamics of time-resolved social interactions

Alessio Cardillo,[1,2] Giovanni Petri,[3] Vincenzo Nicosia,[4] Roberta Sinatra,[5] Jesús Gómez-Gardeñes,[1,2] and Vito Latora[4,6]

[1] *Departmento de Física de la Materia Condensada, Universidad de Zaragoza, E-50009 Zaragoza, Spain*
[2] *Institute for Biocomputation and Physics of Complex Systems (BIFI), University of Zaragoza, E-50018 Zaragoza, Spain*
[3] *Institute for Scientific Interchange (ISI), via Alassio 11/c, 10126 Torino, Italy*
[4] *School of Mathematical Sciences, Queen Mary University of London, London, UK*
[5] *Center for Complex Network Research and Department of Physics, Northeastern University, Boston, MA 02115, USA*
[6] *Dipartimento di Fisica e Astronomia, Università di Catania, and INFN, Via S. Sofia 64, I-95123 Catania, Italy*

Cooperation among unrelated individuals is frequently observed in social groups when their members join efforts and resources to obtain a shared benefit which is unachievable by singles. However, understanding why cooperation arises despite the natural tendency of individuals towards selfish behaviors is still an open problem and represents one of the most fascinating challenges in evolutionary dynamics. Very recently, the structural characterization of the networks upon which social interactions take place has shed some light on the mechanisms by which cooperative behaviours emerge and eventually overcome the individual temptation to defect. In particular, it has been found that the heterogeneity in the number of social ties and the presence of tightly-knit communities lead to a significant increase of cooperation as compared with the unstructured and homogeneous connection patterns considered in classical evolutionary dynamics. Here we investigate the role of social ties dynamics for the emergence of cooperation in a family of social dilemmas. Social interactions are in fact intrinsically dynamic, fluctuating and intermitting over time, and can be represented by time-varying networks, that is graphs where connections between nodes appear, disappear, or are rewired over time. By considering two experimental data sets of human interactions with detailed time information, we show that the temporal dynamics of social ties has a profound dramatic impact on the evolution of cooperation: the observed dynamics of pairwise interactions tend to favor selfish behaviors.

arXiv:1302.0558v1 [physics.soc-ph] 4 Feb 2013

The organizational principles driving the evolution and development of natural and social large-scale systems, including populations of bacteria, ant colonies, herds of predators and human societies, rely on the cooperation of a large population of unrelated agents [1–3]. Even if cooperation seems to be a ubiquitous property of social systems, its spontaneous emergence is still a puzzle for scientists since cooperative behaviors are constantly threatened by the natural tendency of individuals towards self-preservation and the never-ceasing competition among agents for resources and success. The preference of selfishness over cooperation is also due to the higher short-term benefits that a single (defector) agent obtains by taking advantage of the efforts of cooperating agents. Obviously, the imitation of such selfish (but rational) conduct drives the system towards a state in which the higher benefits associated to cooperation are no longer achievable, with dramatic consequences for the whole population. Consequently, the relevant question to adress is why cooperative behaviors are so common, and which are the circumstances and the mechanisms that allow them to emerge and persist.

In the last decades, the study of the elementary mechanisms fostering the emergence of cooperation in populations subjected to evolutionary dynamics has attracted a lot of interest in ecology, biology and social sciences [4, 5]. The problem has been tackled through the formulation of simple games that neglect the microscopic differences among distinct social and natural systems, thus providing a general framework for the analysis of evolutionary dynamics [6–8]. Most of the classical models studied within this framework made the simplifying assumption that social systems are characterized by homogeneous structures, in which the interaction probability is equal for any pair of agents and constant over time [9]. However, this assumption has been proven false for real systems, as the theory of complex networks has revealed that most natural and social networks exhibit large heterogeneity and non–trivial interconnection topologies [10–13]. It has been also shown that the structure of a network has dramatic effects on the dynamics of processes taking place on it, so that complex network analysis has become a fundamental tool in epidemiology, computer science, neuroscience and social sciences [14–16].

The study of evolutionary games on complex topologies has allowed a new way out for cooperation to survive in some paradigmatic cases such as the Prisoner's Dilemma [17–19] or the Public Goods games [20, 21]. In particular, it has been pointed out that the complex patterns of interactions among the agents found in real social networks, such as scale-free distributions of the number of contacts per individual or the presence of tightly-knit social groups, tend to favor the emergence and persistence of cooperation. This line of research, which brings to-

gether the tools and methods from the statistical mechanics of complex networks and the classical models of evolutionary game dynamics, has effectively became a new discipline, known as Evolutionary Graph Theory [22–25].

Recently, the availability of longitudinal spatio-temporal information about human interactions and social relationships [26–29] has revealed that social systems are not static objects at all: contacts among individuals are usually volatile and fluctuate over time [30, 31], face-to-face interactions are bursty and intermittent[32, 33], agents motion exhibits long spatio-temporal correlations [34–36]. Consequently, static networks, constructed by aggregating in a single graph all the interactions observed among a group of individuals across a given period, can be only considered as simplified models of real networked systems. For this reason, time-varying graphs have been lately introduced as a more realistic framework to encode time-dependent relationships [37–41]. In particular, a time-varying graph is an ordered sequence of graphs defined over a fixed number of nodes, where each graph in the sequence aggregates all the edges observed among the nodes within a certain temporal interval. The introduction of time as a new dimension of the graph provides a richer structure. Therefore, new metrics specifically designed to characterize the temporal properties of graph sequences have been proposed and most of the classical metrics defined for static graphs have been extended to the time-varying case [41–46]. Lately, the study of dynamical processes taking place on time-evolving graphs has shown that temporal correlations and contact recurrence play a fundamental role in diverse settings such as random walks dynamics [47, 48], the spreading of information and diseases [49–51] and synchronization [52].

Here we study how the level of cooperation is affected by taking into account the more realistic picture of social system provided by time-varying graphs instead of the classical (static) network representation of interactions. We consider a family of social dilemmas, including the Hawk-Dove, the Stag Hunt and the Prisoner's dilemma games, played by agents connected through a time-evolving topology obtained from real traces of human interactions. We analyze the effect of temporal resolution and correlations on the emergence of cooperation in two paradigmatic data sets of human proximity, namely the MIT Reality Mining [26] and the INFOCOM'06 [27] co-location traces. We found that the level of cooperation achievable on time-varying graphs crucially depends on the temporal resolution at work, i.e. on the length of the aggregation interval used to construct each graph in the sequence. In particular, larger aggregation intervals tend to promote cooperation while smaller time-scales favor defectors. Furthermore, the temporal ordering of interactions hinders cooperation, so that temporally reshuffled versions of the same time-varying graph usually exhibit a considerably higher level of cooperation. Finally, we show that the average size of the giant component across different consecutive time-windows is indeed a good predictor of the level of cooperation attainable on time-varying graphs.

I. RESULTS

A. Evolutionary Dynamics of Social Dilemmas

We focus on the emergence of cooperation in systems whose individuals face a social dilemma between two possible strategies: *Cooperation* (C) and *Defection* (D). A large class of social dilemmas can be formulated as in [18] via a two-parameter game described by the payoff matrix:

$$\begin{array}{cc} & \begin{array}{cc} C & D \end{array} \\ \begin{array}{c} C \\ D \end{array} & \begin{pmatrix} R & S \\ T & P \end{pmatrix} \end{array} = \begin{array}{cc} & \begin{array}{cc} C & D \end{array} \\ \begin{array}{c} C \\ D \end{array} & \begin{pmatrix} 1 & S \\ T & 0 \end{pmatrix} \end{array}, \tag{1}$$

where R, S, T and P represent the payoffs corresponding to the various possible encounters between two players. Namely, when the two players choose to cooperate they both receive a payoff $R = 1$ (for *Reward*), while if they both decide to defect they get $P = 0$ (for *Punishment*). When a cooperator faces a defector it gets the payoff S (for *Sucker*) while the defector gets T (for *Temptation*). In this version of the game the payoffs S and T are the only two free parameters of the model, and their respective values induce an ordering of the four payoffs which determines the type of social dilemma. We have in fact three different scenarios. When $T > 1$ and $S > 0$, defecting against a cooperator provides the largest payoff, and this corresponds to the *Hawk-Dove* game. For $T < 1$ and $S < 0$, cooperating with a defector is the worst case, and we have the *Stag Hunt* game. Finally, for $T > 1$ and $S < 0$, when a defector plays with a cooperator we have at the same time the largest (for the defector) and the smallest (for the cooperator) payoffs, and the game corresponds to the *Prisoner's Dilemma*. In this work we consider the three types of games by exploring the parameter region $T \in [0, 2]$ and $S \in [-1, 1]$.

In real social systems, each individual has more than one social contact at the same time. This situation is usually represented [24] by associating each player i, $i = 1, 2, \ldots, N$ to a node of a *static* network with adjacency matrix $A = \{a_{ij}\}$, whose edges indicate pairs of individuals playing the game. In this framework, a player i selects a strategy, plays a number of games equal to the number of her neighbors $k_i = \sum_j a_{ij}$ and accumulates the payoffs associated to each of these interactions. Obviously, the outcome of playing with a neighbor depends both on the strategy selected by node i and on that of the neighbor, according to the payoff matrix in Eq. 1. After all the individuals have played with all their neighbors in the network, they update their strategies as a result of an evolutionary process, i.e., according to the total collected payoff. Namely, each individual i compares her cumulated payoff p_i with that of one of her neighbors, say j, chosen at random. The probability $P_{i\to j}$ that agent i

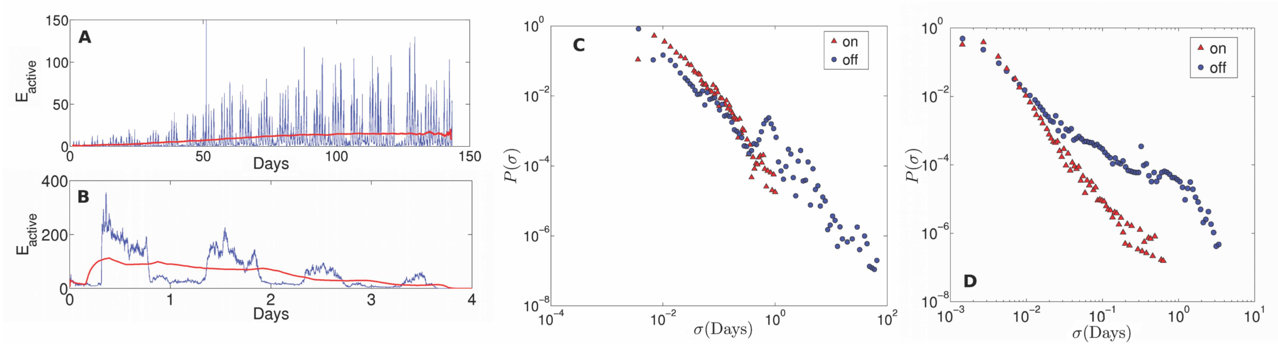

FIG. 1. **Activity patterns of human interactions.** The number E_{active} of links in the graph at time t is reported as a function of time (blue) for MIT Reality Mining **(A)** and INFOCOM'06 **(B)**. Weekly and daily periodicities are visible. Moving averages (red), respectively over a 1-month window and a 1-day window, reveal the non-stationarity of the sequences. The time distributions of edge active and inactive periods (respectively triangles and circles) for MIT Reality Mining **(C)** and INFOCOM'06 **(D)** The data were log-binned. The peak at $\sigma \sim 1$ for the inactive periods corresponds to 24 hours.

adopts the strategy of her neighbor j increases with the difference $(p_j - p_i)$ (see Methods for details).

The games defined by the payoff matrix in Eq. 1 and using a payoff-based strategy update rule have been thoroughly investigated in static networks with different topologies. The main result is that when the network is fixed and agent strategies are allowed to evolve over time, the level of cooperation increases with the heterogeneity of the degree distribution of the network, being scale-free networks the most paradigmatic promoters of cooperation [17–19]. However, in most cases human contacts and social interactions are intrinsically dynamic and varying in time, a feature which has profound consequences on any process taking place over a social network. We explore here the role of time on the emergence of cooperation in time-varying networks.

B. Temporal patterns of social interactions

We consider two data sets describing the temporal patterns of human interactions at two different time scales. The first data set has been collected during the MIT Reality Mining experiment [26], and includes information about spatial proximity of a group of students, staff, and faculty members at the Massachusetts Institute of Technology, over a period of six months. The resulting time-dependent network has $N = 100$ nodes and consists of a time-ordered sequence $\{G_1, G_2, \ldots, G_M\}$ of $M = 41291$ graphs (snapshots), each graph representing proximity interactions during a time interval of $\tau = 5$ minutes. Remember that each graph $G_m, m = 1, \ldots, M$ accounts for all the instantaneous interactions taking place in the temporal interval $[(m-1)\tau, m\tau]$. The second data set describes co-location patterns, over a period of four days, between the participants of the INFOCOM'06 conference [27]. In this case, the resulting time-dependent network has $N = 78$ nodes, and contains a sequence of $M = 2880$ graphs obtained by detecting users co-location every $\tau = 2$ minutes.

The frequency of social contacts is illustrated in Fig. 1 (panels A and B), where we report the number of active links at time t, E_{active}, as a function of time. In the MIT Reality Mining data set, social activity exhibits daily and weekly periodicities, respectively due to home-work and working days-weekends cycles. In addition to these rhythms, we notice a non-stationary behavior which is clearly visible when we plot the activity averaged over a 1-month moving window (red line in panel A). In the INFOCOM'06 data set we observe a daily periodicity and a non-stationary trend which is due, in this case, to a decreasing social activity in the last days of the conference as seen by aggregating activity over 24 hours (red line in panel B). We also report in Fig. 1 (panels C and D) the distributions $P(\sigma)$ of contact duration, $\sigma \equiv \sigma_{on}$, and of inter-contact time, $\sigma \equiv \sigma_{off}$ (i.e. the interval between two consecutive appearances of an edge). As it is often the case for human dynamics [32], the distributions of contact duration and inter-contact time are heterogeneous. For the MIT data set, an active edge can persist up to an entire day, while inactive intervals can last over multiple days and weeks; similar patterns are observed in the INFOCOM'06 data set, where some edges remain active up to one entire day and inter-contact times span almost the whole observation interval. Edge activity exhibits significant correlations over long periods of time. In particular, the autocorrelation function of the time series of edge activity shows a slow decay, up to lags of $10-12$ hours for the MIT data set, and of $6-8$ hours for INFOCOM'06, after which the daily periodicity becomes dominant (figure not reported).

C. Evolution of Cooperation in Time-varying Networks

To simulate the game on a time-varying topology $\{G_m\}_{m=1,\ldots,M}$, we start from a random distribution of

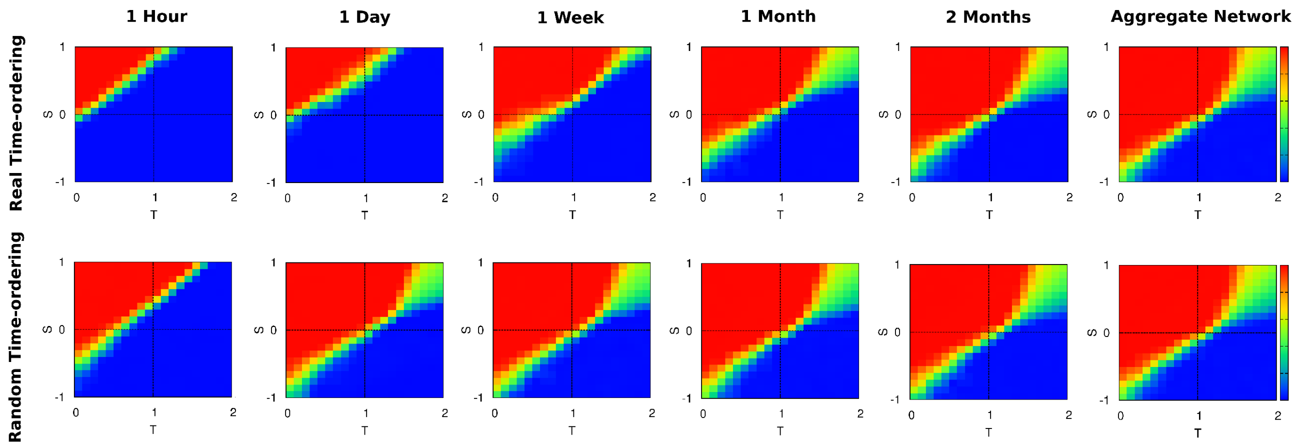

FIG. 2. **Cooperation diagrams for the MIT Reality Mining data set**. Fraction of cooperators at the equilibrium as a function of the temptation to defect (T) and of the sucker's score (S) for different values of the interval Δt between two successive strategy updates. From left to right, the diagrams correspond to Δt equal to 1 hour, 1 day, 1 week, 1 month, 2 months, and to the entire observation period $M\tau \simeq 5$ months. The diagrams in the top row correspond to time-varying graphs with original time ordering, while those in the bottom row are obtained for the same values of Δt but on randomized time-varying graphs. The results are averaged over 50 different realizations. Red corresponds to 100% of cooperators while blue indicates 100% defectors.

strategies, so that each individual initially behaves either as a cooperator or as a defector, with equal probability. The simulation proceeds in *rounds*, where each round consists of a *playing* stage followed by a *strategy update*. In the first stage, each agent plays with all her neighbors on the first graph of the sequence, namely on G_1, and accumulates the payoff according to the matrix in Eq. 1. Then the graph changes, and the agents employ the same strategies to play with all their neighbors in the second graph of the sequence, G_2. The new payoffs are summed to those obtained in the previous iteration. The same procedure is then repeated n times with n such that $n \cdot \tau$ is equal to a chosen interval Δt. At this point, the playing stage terminates and agent strategies are updated. Namely, each agent compares the net payoff accumulated during the previous n time steps with that of one of her neighbors chosen at random. In particular, we adopt here the so-called *Fermi Rule* [53, 54] with a parameter $\beta = 1$ (see Methods). We have checked that the results are quite robust, and we obtain qualitatively similar outcomes for a wide range of β. After the agents have updated their strategy, their payoff is reset to 0 and they start another round, during the subsequent time interval of length $\Delta t = n \cdot \tau$, as described above.

To evaluate the degree of cooperation obtained for a given aggregation interval Δt and a pair of values (T, S), we compute the average fraction of cooperators $\langle C(T, S)_{\Delta t} \rangle$:

$$\langle C(T, S)_{\Delta t} \rangle = \frac{1}{Q} \sum_{i=1}^{Q} \frac{N_c^i}{N}, \qquad (2)$$

where N_c^i is the number of cooperators found at time $i \cdot \tau$ and Q is the total number of rounds played. In general, we set Q large enough to guarantee that the system reaches a stationary state.

We have simulated the system using different update intervals Δt. Updating the strategy every Δt corresponds in practice to study cooperation on a weighted graph aggregated at the temporal scale Δt. In particular when Δt is equal to the entire observation period $M\tau$ we get a static weighted graph where each of the edges has a weight proportional to the number of times that edge has been active in any of the temporal snapshots. For the more general case $\Delta t < M\tau$, an increase of Δt corresponds to a coarser temporal representation of the underlying graph dynamics. We focus here on the top panels of Fig. 2 and Fig. 3, where we show how the average fraction of cooperators depends on the parameters S and T and on the length Δt of the strategy update interval. We considered six values of Δt for the MIT Reality Mining data set, from $\Delta t = 1$ hour up to the whole observation interval, and eight values for INFOCOM'06, ranging from minutes up to the aggregate network.

We first notice that the rightmost diagrams in both figures, which correspond to $\Delta t = M\tau$, are in perfect agreement with the results about evolutionary games played on static topologies reported in the literature (see *e.g.* [18, 24]). If we look at the cooperation diagrams obtained by increasing the value of Δt in the original sequences of graphs (top panels of Fig. 2 and Fig. 3), we notice that, for any pair (T, S), a larger update interval corresponds to a higher fraction of cooperators. In particular, for MIT Reality Mining (Fig. 2) the fraction of cooperators increases up until $\Delta t = 2$ months, after which the cooperation diagram is practically indistinguishable from that obtained on the static aggregated graph. For INFOCOM'06, instead, a strategy update

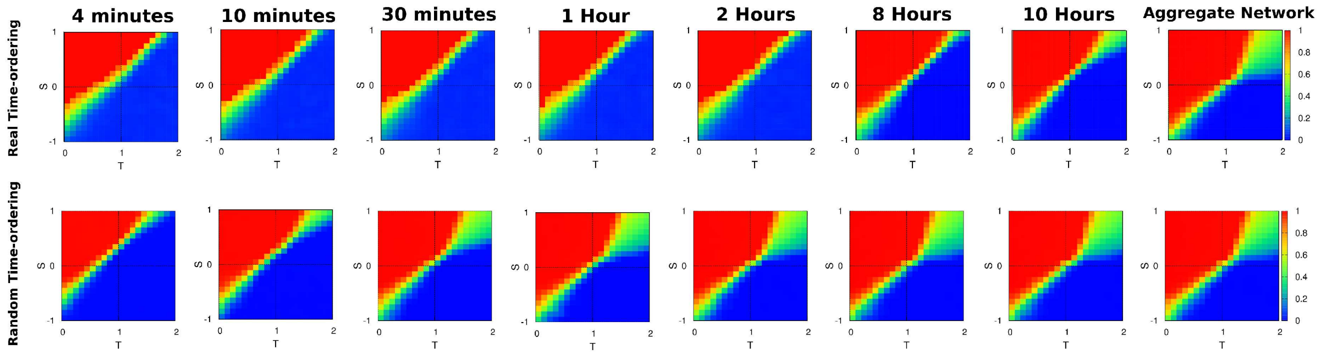

FIG. 3. **Cooperation diagrams for the INFOCOM data set.** Fraction of cooperators at the equilibrium as a function of the temptation to defect (T) and of the sucker's score (S) for different values of the interval Δt between two successive strategy updates. From left to right, the diagrams correspond to Δt equal to 4 minutes, 10 minutes, 30 minutes, 1 hour, 2 hours, 8 hours, 10 hours and $M\tau \simeq 4$ days. The diagrams in the top row correspond to time-varying graphs with original time ordering, while those in the bottom row are obtained for the same values of Δt but on randomized time-varying graphs. The results are averaged over 50 different realizations. Red corresponds to 100% of cooperators while blue indicates 100% defectors.

interval larger than 2 hours already produces a cooperation diagram similar to that obtained in the aggregated graph. These results indicate that defectors actually take advantage from the volatility of edges, and that cooperation can emerge only if the strategy update interval is large enough.

As we pointed out above, edge activation patterns show non-trivial correlations. To highlight the effects of temporal correlations and of periodicity in the appearance of links in the real data sets, we have simulated the games also on randomized time-varying graphs, obtained by uniformly reshuffling the original sequences of snapshots. The results for randomized graphs are reported in the bottom panels of Fig. 2 and Fig. 3. As expected, for $\Delta t = M\tau$ the cooperation diagrams obtained on the reshuffled sequences (bottom rightmost panels of the two figures) are identical to those obtained on the corresponding original data sets (top rightmost panels). In fact, the weight associated to each link in the aggregated graph is equal to the number of times that this link has appeared in the observation interval, and this number is equal for both the original and the reshuffled graph sequences. Conversely, for smaller values of Δt, the weight of a link in each of the smaller aggregated graphs depends on the existence of temporal correlations, namely on the frequency and persistence of the link. By reshuffling the sequence of snapshots these correlations are washed out, so that when $\Delta t = 1$ week and $\Delta t = 1$ hour, respectively for MIT Reality Mining and INFOCOM'06, the cooperation diagram becomes comparable with that obtained on the aggregated graph.

The results reported in Fig. 2 and Fig. 3 suggest that the number of edges in each time-window, the persistence of edges over several consecutive time-windows and their periodicity are all fundamental to discourage defectors. When Δt is small each aggregated graph is sparse and agents are connected, on average, to a small neighborhood. If edges persist over time, in the long run the majority of agents will prefer to defect. In fact, the cooperating neighbors of a defector will tend to retaliate on it when they update their strategies (i.e. they will turn into defectors). Thus, if each graph is too sparse and edges persist over subsequent graph, defectors easily prevail on cooperators. Conversely, when Δt is large then each aggregated graph is more dense, and the presence and persistence of triangles will discourage defectors and enhance cooperation. In fact, the study of cooperation in static graphs with tunable clustering coefficient has revealed that the presence of closed triangles strongly foster cooperation [55].

When we consider randomized sequences of snapshots, for each value of Δ, all the aggregated graphs have a similar density of links, while the density is more heterogeneously distributed among the randomized sequence than that of the original sequence. In the graphs obtained by randomizing the original sequence, a link appears in each aggregated graph, on average, with the same frequency at which it appears in the whole sequence. Thus, when Δt is large enough, the distribution of edge weights in each graph is similar to that of the aggregated graph corresponding to $\Delta t = M\tau$ so that results become indentical to those obtained on top of the corresponding static graph.

D. Structural analysis of time varying networks

In order to understand the dependence of cooperation on the structural properties of the graphs at different aggregation scales, we plot in Fig. 4 the average fraction$\langle \mathcal{S} \rangle$ of the nodes found in the giant component of the graphs as a function of Δt, for the original and for the reshuffled sequences of snapshots. In general, for a given value of Δt the giant component of graphs corresponding to randomized sequences is larger than that of graphs obtained from the original ordering. In Fig. 4 we also plot the

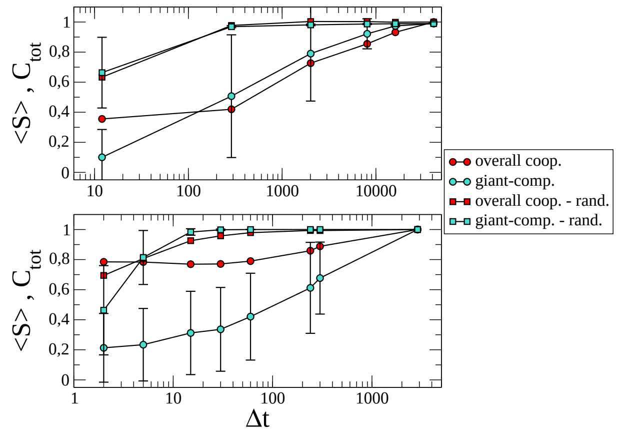

FIG. 4. **Cooperation level and size of the Giant Component**. Average size of the giant component $\langle \mathcal{S} \rangle$ and overall cooperation level $C_{tot}(\Delta t)$ as a function of the aggregation interval Δt for MIT Reality Mining (top panel) and INFOCOM'06 (bottom panel). Black circles and red squares correspond, respectively, to the original sequences of graphs and to the uniformly reshuffled sequences. Error bars indecate the standard deviation of $\langle \mathcal{S} \rangle$ across the sequence of graphs.

overall level of cooperation at a given aggregation scale Δt, $C_{tot}(\Delta t)$, defined as:

$$C_{tot}(\Delta t) = \frac{1}{C_{tot}(M\tau)} \int_0^2 \mathrm{d}T \int_{-1}^1 C(T,S)\mathrm{d}S$$

Notice that $C_{tot}(\Delta t)$ is divided by the value $C_{tot}(M\tau)$ corresponding to the whole observation interval, so that $C_{tot} \in [0,1]$. The value of Δt at which $\langle \mathcal{S} \rangle$ is comparable with the number of nodes, i.e. when $\langle \mathcal{S} \rangle \simeq 1$, coincides with the value of Δt at which the cooperation diagram becomes indistinguishable from that obtained for the aggregate network, $C_{tot}(\Delta t) \simeq 1$, for both the original and the reshuffled sequences of snapshots. This result confirms that the size of the giant connected component of the graph corresponding to a given aggregation interval plays a central role in determining the level of cooperation sustainable by the system, in agreement with the experiments discussed in [56] for the case of static graphs.

II. CONCLUSIONS

Although the impact of network topology on the emergence and persistence of cooperation has been extensively studied in the last years, the recent availability of data sets with time-resolved information about social interactions allows a deeper investigation of the impact on evolutionary dynamics of time-evolving social structures. Here we have addressed a crucial question: does time resolution affects the classical results about the enhancement of cooperation driven by network reciprocity? The results of the simulations confirm that the resilience of cooperation is hindered when high-resolution time-varying graphs are considered. In particular, high temporal resolution strongly affects the persistence of cooperation in all the paradigmatic social dilemmas. This phenomenon is a consequence of the relatively small size of the giant component of the graphs obtained at small aggregation intervals. However, when the temporal sequence of social contacts is randomly reshuffled, the average size of the giant component of aggregated graphs increases, and the effects of temporal resolution over cooperation are smoothed. As a result, cooperation can emerge and persist also for moderately high time resolutions. Thus, not only temporal resolution but also temporal correlations across consecutive snapshots are fundamental for cooperation to emerge.

Our findings suggest that the frequency at which the connectivity of a given system are sampled has to be carefully chosen, according with the typical time-scale of the social interaction dynamics. For instance, as stock brokers might decide to change strategy after just a couple of interactions, other processes like trust formation in business or collaboration networks are likely to be better described as the result of multiple subsequent interactions.

In a nutshell, the arguments indicating network reciprocity as the social promotor of cooperator have to be revisited when considering time-varying graphs. In particular, one should always bear in mind that both the over- and the under-sampling of time-evolving social graph and the use of the finest/coarsest temporal resolution could substantially bias the results of a game-theoretic model played on the corresponding network. These results pave the way to a more detailed investigation of social dilemmas in systems where not only structural but also temporal correlations are incorporated in the interaction maps.

III. METHODS

A. MIT Reality Minining data set

The data set describes proximity interactions collected through the use of Bluetooth-enabled phones [26]. The phones were distributed to a group of 100 users, composed by 75 MIT Media Laboratory students and 25 faculty members. Each device had a unique tag and was able to detect the presence and identity of other devices within a range of 5-10 meters. The interactions, intended as proximity of devices, were recorded over a period of about six months. In addition to the interaction data, the original dataset included also information regarding call logs, other Bluetooth devices within detection range, the cell tower to which the phones was connected and information about phone usage and status. Here, we consider only the contact network data, ignoring any other contextual metadata. The resulting time-varying network is an ordered sequence of 41291 graphs, each having N=100 nodes. Each graph corresponds to a proximity scan taken

every 5 minutes. An edge between two nodes indicates that the two corresponding devices were within detection range of each other during that interval. We refer to such links as *active*. During the entire recorded period, 2114 different edges have been detected as active, at least once. This corresponds to the aggregate graph having a large average node degree $\langle k \rangle \simeq 42$. However, this is an artefact of the aggregation; the single snapshots tend to be very sparse, usually containing between 100 and 200 active edges.

B. INFOCOM'06 data set

The data set consists of proximity measurements collected during the IEEE INFOCOM'06 conference held in a hotel in Barcelona in 2006 [27]. A sample of 78 participants from a range of different companies and institutions were chosen and equipped with a portable Bluetooth device, Intel iMote, able to detect similar devices nearby. Area "inquiries" were performed by the devices every 2 minutes, with a random delay or anticipation of 20 seconds. The delay/anticipation mechanism was implemented in order to avoid synchronous measurements, because, while actively sweeping the area, devices could not be detected by other devices. A total number of 2730 distinct edges were recorded as active at least once in the observation interval, while the number of edges active at a given time is significantly lower, varying between 0 and 200, depending on the time of the day.

C. Strategy update rule

The Fermi Rule consists in the following updating strategy. A player i chooses one of her neighbors j at random and copies the strategy of j with a probability:

$$P_{i\to j} = \frac{1}{1 + e^{-\beta(p_j - p_i)}} \ , \qquad (3)$$

where $(p_j - p_i)$ is the difference between the payoffs of the two players, and β is a parameter controlling the smoothness of the transition from $P_{i\to j} = 0$ for small values of $(p_j - p_i)$, to $P_{i\to j} = 1$ for large values of $(p_j - p_i)$. Notice that for $\beta \ll 1$ we obtain $P_{i\to j} \simeq 0.5$ regardless of the value of $(p_j - p_i)$, which effectively corresponds to a random strategy update. On the other hand, when $\beta \gg 1$ then $P_{i\to j} \simeq \Theta(p_j - p_i)$, being $\Theta(x)$ the Heaviside step function. In this limit, the strategy update is driven only by the ordering of the payoff values.

ACKNOWLEDGMENTS

This work was supported by the EU LASAGNE Project, Contract No.318132 (STREP), by the EU MULTIPLEX Project, Contract No.317532 (STREP), by the Spanish MINECO under projects MTM2009-13848 and FIS2011-25167 (co-financed by FEDER funds), by the Comunidad de Aragón (Grupo FENOL) and by the Italian TO61 INFN project. J.G.G. is supported by Spanish MINECO through the Ramón y Cajal program. G.P. is supported by the FET project "TOPDRIM" (IST-318121). R.S. is supported by the James S. McDonnell Foundation.

[1] Pennisi E (2005) How did cooperative behavior evolve? *Science* 309: 93.
[2] Pennisi E (2009) On the origin of cooperation. *Science* 325: 1196–1199.
[3] Maynard-Smith J, Szathmary E (1995) *The Major Transitions in Evolution* (Freeman, Oxford, UK).
[4] Nowak MA (2006) *Evolutionary dynamics: exploring the equations of life* (The Belknap Press of Harvard University Press, Cambridge, MA)
[5] Kollock P (1998) Social dilemmas: the anatomy of cooperation. *Annu. Rev. Sociol.* 24: 183–214.
[6] Maynard-Smith J, Price G R (1973) The logic of animal conflict, *Nature* 246: 5427.
[7] Maynard-Smith J (1982) *Evolution and the Theory of Games* (Cambridge Univ. Press, Cambridge, UK).
[8] Gintis H (2009) *Game theory evolving* (Princeton University Press, Princeton, NJ).
[9] Samuelson L (2002) Evolution and game theory. *J. Econ. Perspect.* 16(2): 47–66.
[10] Watts DJ, Strogatz SH (1998) Collective dynamics of small-world networks. *Nature* 393: 440-442.
[11] Strogatz SH (2001) Exploring complex networks. *Nature* 410: 268-276.
[12] Albert R, Barabási A-L (2002) Statistical mechanics of complex networks. *Rev. Mod. Phys.* 74: 47–97 (2002).
[13] Newman MEJ (2003) The Structure and Function of Complex Networks. *SIAM Rev.* 45: 167–256.
[14] Boccaletti S, Latora V, Moreno Y, Chavez M, Hwang D-U (2006) Complex Networks: Structure and Dynamics. *Phys. Rep.* 424: 175–308.
[15] Dorogovtsev SN, Goltsev AV, Mendes JFF (2008) Critical phenomena in complex networks *Rev Mod. Phys.* 80: 1275–1335.
[16] Castellano C, Fortunato S, Loreto V (2009) Statistical physics of social dynamics. *Rev. Mod. Phys.* 81: 591–646.
[17] Santos FC, Pacheco JM (2005) Scale-Free Networks Provide a Unifying Framework for the Emergence of Cooperation. *Phys. Rev. Lett.* 95: 098104.
[18] Santos FC, Pacheco JM, Lenaerts T (2006) Evolutionary dynamics of social dilemmas in structured heterogeneous populations. *Proc. Natl. Acad. Sci. U.S.A.* 103: 3490–3494.

[19] Gómez-Gardeñes J, Campillo M, Floría LM, Moreno Y (2007) Dynamical Organization of Cooperation in Complex Topologies. *Phys. Rev. Lett.* 98: 108103.

[20] Santos FC, Santos MD, Pacheco JM (2008) Social diversity promotes the emergence of cooperation in public goods games. *Nature* 454: 213–216.

[21] Gómez-Gardeñes J, Romance M, Criado R, Vilone D, Sánchez A (2011) Evolutionary games defined at the network mesoscale: The Public Goods game. *Chaos* 21: 016113.

[22] Szabó G, Fáth G (2007) Evolutionary games on graphs. *Phys. Rep.* 447: 97.

[23] Jackson MO (2008) *Social and economic networks* (Princeton Univ. Press, Princeton, NJ).

[24] Roca CP, Cuesta J, and Sánchez A (2009) Evolutionary game theory: temporal and spatial effects beyond replicator dynamics. *Phys. Life Rev.* 6: 208.

[25] Perc M, Szolnoki A (2010) Coevolutionary games - A mini review. *BioSystems* 99: 109–125.

[26] Eagle, N, Pentland, A. (2006) Reality mining: sensing complex social systems. *Personal and Ubiquitous Computing*, 10(4), 255–268.

[27] J. Scott et al., CRAWDAD Trace (INFOCOM, Barcelona, 2006).

[28] Isella L, Romano M, Barrat A, Cattuto C, Colizza V, et al. (2011) Close Encounters in a Pediatric Ward: Measuring Face-to-Face Proximity and Mixing Patterns with Wearable Sensors. *PLoS ONE* 6(2):e17144.

[29] Stehle J, Voirin N, Barrat A, Cattuto C, Isella L, et al. (2011) High-Resolution Measurements of Face-to-Face Contact Patterns in a Primary School. *PLoS ONE* 6(8): e23176.

[30] Isella L, Stehlé J, Barrat A, Cattuto C, Pinton J-F, Van den Broeck, W (2011) What's in a crowd? Analysis of face-to-face behavioral networks. *J. Theor. Biol.* 271: 166–180.

[31] Karsai M, Kivel Mä, Pan RK, Kaski K, Kertész J, Barabási AL, Saramäki J (2011) Small But Slow World: How Network Topology and Burstiness Slow Down Spreading *Phys. Rev. E* 83: 025102(R).

[32] Barabási, A-L (2005) The origin of bursts and heavy tails in human dynamics. *Nature* 435: 207–211.

[33] Stehlé J, Barrat A, Bianconi G (2010) Dynamical and bursty interactions in social networks. *Phys. Rev. E* 81:035101(R) (2010).

[34] González MC, Hidalgo CA, Barabási A-L (2008) Understanding individual human mobility patterns. *Nature* 453: 779–782.

[35] Szell M, Lambiotte R, Thurner S (2010) Multi-relational Organization of Large-scale Social Networks in an Online World. *Proc. Natl. Acad. Sci. U.S.A.* 107: 13636–13641.

[36] Szell M, Sinatra R, Petri G, Thurner S, Latora V (2012) Understanding mobility in a social petri dish *Scientific Reports* 2: 457.

[37] Kossinets G, Kleinberg J, Watts D (2008) The Structure of Information Pathways in a Social Communication Network, *Proc. 14th ACM SIGKDD Intl. Conf. on Knowledge Discovery and Data Mining*

[38] Kostakos, V. (2009) Temporal graphs. *Physica A* 388(6): 1007–1023.

[39] Tang J, Musolesi M, Mascolo C, Latora V (2009) Temporal Distance Metrics for Social Network Analysis *Proceedings of the 2nd ACM SIGCOMM Workshop on Online Social Networks (WOSN'09)*

[40] Holme P, Saramäki J (2011) Temporal networks *arXiv:1108.1780v2*

[41] Tang J, Scellato S, Musolesi M, Mascolo C, Latora V (2010), *Phys. Rev. E* 81: 055101(R).

[42] Pan RK, Saramäki J (2011) Path lengths, correlations, and centrality in temporal networks, *Phys. Rev. E* 84: 016105.

[43] Kovanen L, Karsai M, Kaski K, Kertesz J, Saramäki J (2011) Temporal motifs in time-dependent networks. *J. Stat. Mech.* P11005.

[44] Tang J, Musolesi M, Mascolo C, Latora V, Nicosia V (2010) Analysing Information Flows and Key Mediators through Temporal Centrality Metrics *Proceedings of the 3rd ACM Workshop on Social Network Systems (SNS'10).*

[45] Nicosia V, Tang J, Musolesi M, Russo G, Mascolo C, Latora V (2012) Components in time-varying graphs *Chaos* 22: 023101.

[46] Mucha PJ, Richardson T, Macon K, Porter MA, Onnela J-P (2010) Community structure in time-dependent, multiscale, and multiplex networks. *Science* 328: 876–878.

[47] Starnini M, Baronchelli A, Barrat A, Pastor-Satorras R (2012) Random walks on temporal networks *Phys. Rev. E* 85, 056115

[48] Perra N, Baronchelli A, Mocanu D, Goncalves B, Pastor-Satorras R, Vespignani A (2012) Walking and searching in time-varying networks arXiv:1206.2858.

[49] Rocha LEC, Liljeros F, Holme P (2011) Simulated Epidemics in an Empirical Spatiotemporal Network of 50,185 Sexual Contacts. *PLoS Comput Biol* 7(3): e1001109.

[50] Rocha LEC, Decuyper A, Blondel VD (2012) Epidemics on a stochastic model of temporal network *arXiv:1204.5421.*

[51] Rocha LEC, Blondel VD (2012) Temporal heterogeneities increase the prevalence of epidemics on evolving networks *arXiv:1206.6036*

[52] Fujiwara N, Kurths J, Díaz-Guilera A (2011) Synchronization in networks of mobile oscillators *Phys. Rev. E* 83, 025101(R).

[53] Blume, L.E. (1993) The Statistical Mechanics of Strategic Interaction. *Games Econ. Behav.* 5: 387.

[54] Szabó, G., and Töke, C. (1998) Evolutionary prisoner's dilemma game on a square lattice. *Phys. Rev. E* **58**: 69

[55] Assenza, S., Gómez-Gardeñes, J., and Latora V. (2008) Enhancement of cooperation in highly clustered scale-free networks. *Phys. Rev. E* 78: 017101.

[56] Wang, Z., Szolnoki, A., and Perc, M. (2012) If players are sparse social dilemmas are too: Importance of percolation for evolution of cooperation. *Sci. Reports* 2, 369.